Implantation of keV-energy argon clusters and radiation damage in diamond

V. N. Popok[*]

Department of Physics and Nanotechnology, Aalborg University, Skjernvej 4A, DK-9220 Aalborg Øst, Denmark

J. Samela and K. Nordlund

Department of Physics and Helsinki Institute of Physics, University of Helsinki, P.O. Box 43, FI-00014 Helsinki, Finland

V. P. Popov

Institute of Semiconductor Physics, Lavrentieva Avenue 13, 630090 Novosibirsk, Russia

We show that for impacting argon clusters, both mean projected ranges of the constituents and depths of radiation damage in diamond scale linearly with momentum. The same dependence was earlier found for keV-energy cluster implantation in graphite, thus suggesting the universality of this scaling law. For diamond, a good agreement for the value of displacement energy for the case of cluster impact is found by comparing the calculated target sputtering and experimentally measured depth of radiation damage.

Ion-beam technologies have attained an advanced stage of development that was stimulated by the recent trends in research and industry. Along with traditional monomer ion implantation, another approach, namely, the use of cluster ions for material modification, has attracted considerable attention, especially during the last decade.[1–3] Using cluster ion-beam technology, one can control the cluster size (which can vary from a few up to thousands of constituents) and its impact energy. This provides a number of advantages for the modification of surfaces, for example, for ultrashallow junction formation,[1,4,5] infusion doping,[6] dry etching, and smoothing.[1,7]

From the application point of view, it is essential to know all the parameters that affect the stopping of the projectiles and related phenomena in the material. Cluster implantation is significantly different from that of the monatomic projectiles due to the multicomponent structure and relatively weak bonding between atoms in a cluster.[3,8] Collisions of many cluster atoms at a relatively small surface area lead to a high density of energy locally transferred to the target, which causes nonlinear effects, leading to strong radiation damage.[3,9] The primary collision stage affects very much the penetration dynamics of the clusters: cluster constituents have longer ranges compared to monomers at the same impact energy per atom.[10,11] Unfortunately, different simulations and experiments showed rather different dependences of the projected ranges R_p of cluster constituents and radiation damage developed by them for various cluster species, sizes, and energies as well as for different target materials.[3] However, recent experiments of cluster implantation supported by molecular dynamics (MD) simulations demonstrated that a universal dependence of the cluster stopping can be reached at least for graphite.[12,13] It was proved that R_p can be linearly scaled with the square root of cluster kinetic energy E_{kin}, which is proportional to cluster momentum.

In this Brief Report, we present experimental results and MD simulations of argon cluster implantation in diamond and demonstrate that the mean R_p of cluster constituents and depth of the damage introduced by them follow the above-mentioned linear dependence on the cluster momentum. The interest in diamond comes from its electronic characteristics, for instance, the high mobility of electrons and holes, low noise and leakage current, and extremely high thermal conductivity that make this material attractive for high-power and high-frequency electronics.[14] Diamond also is a potential platform of solid-state quantum devices.[15]

Small (with an area of a few mm^2) 1-mm thick plates of (111) synthetic diamond were used for the experiments. The samples were implanted by Ar$_n^+$ cluster ions using the pulsed cluster source together with the cluster implantation and deposition apparatus.[16,17] One of the samples was bombarded by an entire spectrum of sizes (n is from 1 up to ∼80 atoms) with energy of 4 keV/cluster and total fluence of about 10^{11} cm^{-2}. Other samples were implanted by size-selected Ar$_{27\pm2}^+$ cluster ions with energies of 9, 12, and 15 keV/cluster ($E_{at} \approx$ 333, 444, 555 eV/atom, respectively) at fluences of ∼10^{10} cm^{-2}. After implantation the samples were exposed to two stages of treatment. The first one was conventional furnace annealing at 600 °C for 5–10 min. The annealing was carried out in ambient atmosphere. The second one combined chemical processing with thermal annealing. The samples were kept in a 10% water solution of KNO$_3$ for 15 min, then heated up to 100 °C for 15 min in order to dry them, and finally annealed at 380 °C for 15 min in ambient atmosphere to remove products of the chemical reaction. Both stages were intended to provide etching of radiation-damaged areas caused by the cluster collisions.

Surfaces of the samples were studied *ex situ* after each of the above-mentioned stages, i.e., the implantation, thermal annealing, and combined processing, using atomic force microscopy (AFM). AFM investigations were carried out in tapping mode by Probe Nano Laboratory NTEGRA (from NT-MDT). Commercial cantilevers with ultrasharp silicon or diamond-like carbon tips (curvature radius of 1–3 nm) were utilized.

Classical MD simulations were performed using the PARCAS simulation software[18] and the Tersoff interatomic potential.[19,20] A Lennard-Jones-type pair potential was used
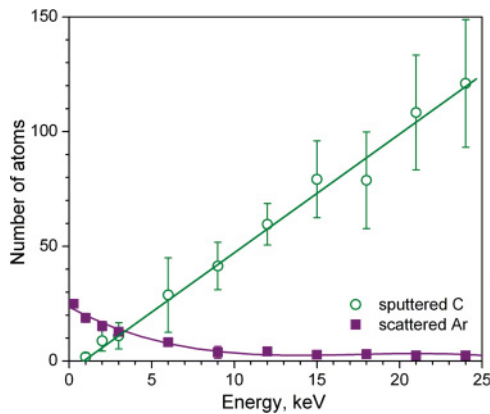
FIG. 1. (Color online) Calculated dependences of the number of sputtered C and scattered Ar atoms on kinetic energy of impacting Ar_{27} clusters.

between the Ar atoms. A short-range repulsive force[21] was also present between all pairs of atoms to better describe collisions between them. The Ar-C interaction was purely repulsive.[22,23] The size of the (111) diamond target in the simulations was $20 \times 20 \times 10$ nm. The borders of the target were cooled, and the simulations were run until the impact area was cooled to the ambient temperature of 300 K (15–25 ps, depending on the cluster energy). Five simulations were performed at each of the energies in the interval between 1 and 27 keV/cluster, varying the initial orientation and position of the impacting Ar_{27} cluster.

For the sample implanted by an entire spectrum of clusters ($E_{kin} = 4$ keV/cluster), the maximum of the size distribution corresponded to $n \approx 25$–30 atoms, thus providing good conditions for comparison with size-selected Ar_{27} clusters. These sizes give mean kinetic energies of $E_{at} \approx 130$–200 eV/atom. It was shown elsewhere that argon clusters with these low energies produce only a small amount of damage on the diamond surface, which could not be registered using AFM.[24] Our MD simulations of Ar_{27} cluster collisions with diamond confirm this finding. They demonstrate that clusters fragment on impact, and some fraction of cluster atoms becomes scattered (Fig. 1). The number of scattered atoms gradually decreases with the increase of E_{kin}. At higher energies there are only a few atoms per cluster that are scattered; the rest become implanted. However, for $E_{kin} = 1$ keV/cluster the scattered fraction is about 2/3, and for 4 keV/cluster it is still considerable, about 1/3. Thus, clusters of these energies can lead only to minimal and shallow damage of diamond.

Thermal annealing of a sample implanted with 4-keV clusters leads to the formation of small bumps, as shown in Fig. 2(a). The surface density of the bumps corresponds well to the cluster fluence. Since the annealing was carried out in ambient atmosphere, one can suggest growth of amorphous carbon structures at the surface spots damaged by the cluster impacts. The following combined chemical and thermal processing causes etching of the amorphized areas, yielding the formation of pits [Fig. 2(b)]. The triangular shape of the pits is related to the crystallographic orientation of diamond. The depth of the pits is expected to correspond to the depth of the radiation damage introduced by the implanted
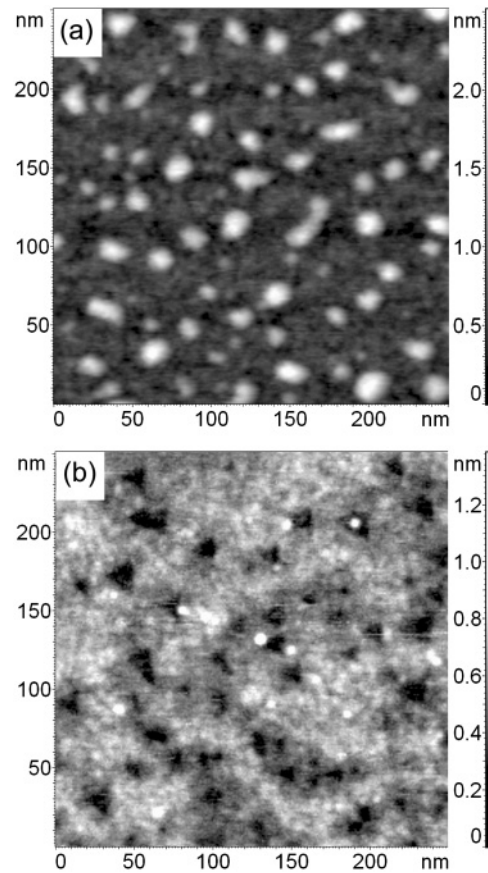

FIG. 2. AFM images of the diamond surface implanted by 4-keV Ar_n clusters (a) after annealing and (b) after combined treatment.

clusters. Similar phenomena of bump formation followed by the conversion into pits under the postimplantation treatment are also observed for the sample implanted by size-selected Ar_{27}^+ clusters ions with $E_{kin} = 9$ keV/cluster.

For the samples bombarded by Ar_{27}^+ cluster ions with E_{kin} of 12 and 15 keV/cluster the formation of small craters or hillocks was experimentally observed.[24] MD simulations show that 12- and 15-keV clusters can sputter from about 60 to 80 carbon atoms, respectively (see Fig. 1). The best fit shows a linear dependence on energy. The line intersects the x axis at a value of about 900 eV, which gives a threshold energy that is required to cause the sputtering. If recalculated per cluster atom it corresponds to ~33 eV. This value is close to the lower limit of the displacement energies (35–80 eV) reported for conventional ion implantation of diamond elsewhere.[25] Thus, for the cluster case, we have evidence of low energy required to displace atoms of the diamond lattice. This low value is related to the multiple-collision effect causing the development of overlapping displacement cascades and the high-energy-density transfer to the diamond target.[26] Similar lowering of the displacement energy was earlier found for the case of argon-cluster implantation in silicon where the decrease was found to be from ~15 eV/atom (conventional monatomic ion implantation) to 4.7 eV/atom for the cluster case.[27]

The implantations with energies of 12 and 15 keV/cluster introduce significant radiation damage, leading to amorphization of the impact areas. The higher level of amorphization
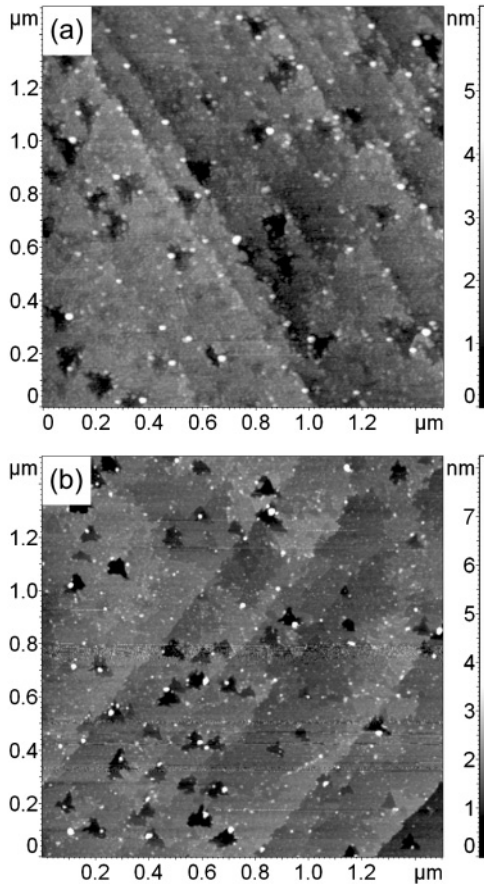
FIG. 3. AFM images of the diamond surface implanted by 15-keV Ar_{27} clusters (a) after annealing and (b) after combined treatment.

of these samples compared to the ones implanted by the lower-energy clusters (4 and 9 keV) leads to the situation where the amorphous carbon can be etched just by the thermal annealing, similar to the case of cluster-implanted graphite.[12,13] At elevated temperatures, carbon atoms undergo chemical reactions with oxygen, yielding volatile compounds. Thus, the triangular pits on the samples implanted with energies of 12 and 15 keV appear directly after the annealing. A typical example of an AFM image can be seen in Fig. 3(a). Subsequent combined chemical and thermal treatment does not change the surface density and depth of the pits [Fig. 3(b)].

Snapshots of MD simulations for impacts of 12- and 15-keV Ar_{27} clusters are presented in Fig. 4. At the beginning of the impact, clusters are broken into individual atoms that penetrate into the target to a certain depth. In the following discussion, we consider mean R_p values of individual projectiles for every cluster impact: these values are presented in Fig. 5. In the experiments, the depth of the etched pits d is measured using AFM. These data are also presented in Fig. 5. As one can see, the dependences can be fitted with the function $a + bE_{\text{kin}}^{1/2}$, where a and b are the fit parameters. The best fit coefficient b is the same for both curves (see Fig. 5). Thus, one can suggest that both d and R_p scale as the square root of energy, which is proportional to cluster momentum for the given cluster size (or mass). The same scaling law was obtained for clusters of various species (Ag, Au, Si, Co, and Ar) and different sizes
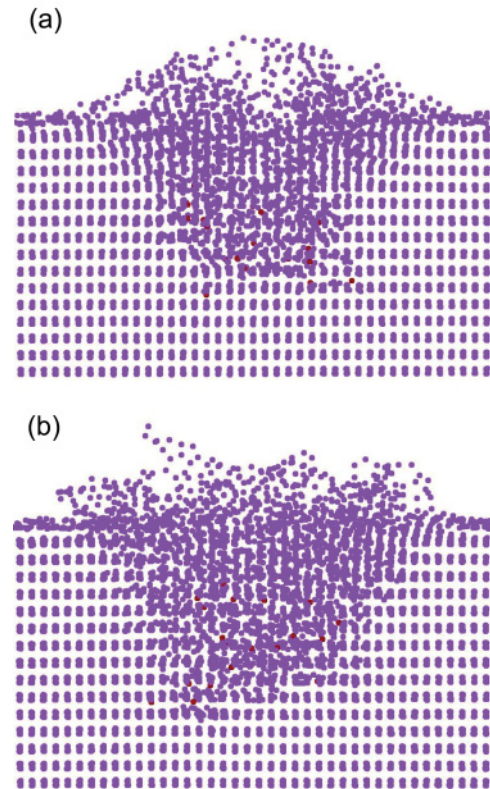

FIG. 4. (Color online) Snapshots of MD simulations (after 15 ps). Implantation of Ar_{27} clusters in diamond with energies of (a) 12 and (b) 15 keV. The width of the frames is 5 nm, and the thickness of the cross sections is 1 nm.

implanted in graphite.[12,13,28] Momentum was found to be an important parameter for understanding the physical picture of cluster stopping in matter.[13] It includes such quantities as velocity and mass. The velocity affects both the development of collision cascades and the final R_p of the constituents. It is worth mentioning that macroscopic bodies have their penetration depths linearly scaled with velocity.[29] Thus, the dependence on velocity creates a "bridge" between collisions
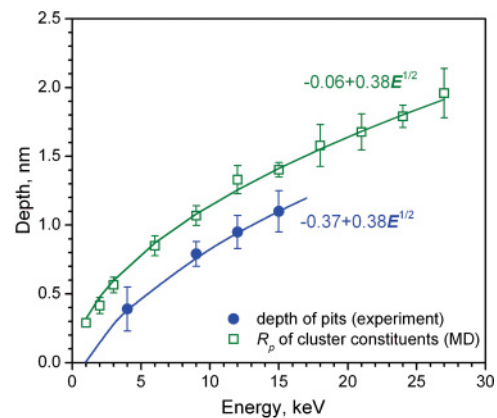

FIG. 5. (Color online) Calculated R_p and experimentally measured d on impact of Ar_n clusters as a function of kinetic energy. For all energies of MD and for 9, 12, and 15 keV of the experiment $n = 27$. For 4 keV of the experiment, maximum cluster size distribution is at $n \approx 25$–30. The best-fit functions are presented for both dependences.

of macroscopic and microscopic objects. The mass of the cluster not only contributes to the stopping and ranges of the projectiles but also defines the cluster-surface interaction area, which is related to the cluster cross section and thus to its size and mass.[12,13] This area is very important for the estimation of the radiation-damaged region formed in the target. The difference in depth between the experimental and simulated curves in Fig. 5 is due to the fact that the depth of the etched pits corresponds to strongly damaged areas of diamond (probably, fully amorphized ones), which is not the same as the mean depth of penetrated cluster constituents. The damage is formed mainly due to the nuclear stopping of the clusters. It is well known from conventional ion implantation that the maximum of the energy loss on nuclear stopping occurs at a depth that is lower compared to the mean projected range.[21] It is also possible that some small amorphous areas introduced at the ends of the trajectories are recrystallized before the etching, thus leading to the lower depth of damage. In our case d is found to be around 0.6–$0.8 R_p$. Another important finding is that the best-fit curve of the experimental data crosses the

x axis at an energy of 948 eV. This energy is very close to the 900 eV reported for the sputtering dependence presented in Fig. 1. Thus, we can suggest a displacement energy of 33–35 eV/atom for Ar_{27} clusters implanted in diamond.

In conclusion, the results obtained on the implantation of argon clusters in diamond show a similarity to the stopping behavior of rare-gas, semiconductor, and metallic clusters in graphite and demonstrate the same scaling law in which both depth of radiation damage and mean projected range of cluster constituents linearly depend on cluster momentum. Comparison of MD simulations on the sputtering of carbon atoms and experimental results on the depth of radiation damage suggests that energies of 33–35 eV/atom are sufficient for the displacement of atoms from their lattice sites in diamond in the case of cluster impact. These values are at the lowest limit of the displacement energies known for conventional monatomic implantation. Hence, this is part of the evidence of the multiple-collision effect leading to the local transfer of high energy from cluster constituents to the target.

[*]vp@nano.aau.dk

[1]N. Toyoda and I. Yamada, IEEE Trans. Plasma Sci. **36**, 1471 (2008).

[2]K. Wegner, P. Piseri, H. V. Tafreshi, and P. Milani, J. Phys. D **39**, R439 (2006).

[3]V. N. Popok, Mater. Sci. Eng. R **72**, 137 (2011).

[4]Y. Kawasaki, M. Ishibashi, M. Kitazawa, Y. Maruyama, S. Endo, T. Yamashita, and T. Kuroi, in *Ion Implantation Technology 2010: 18th International Conference on Ion Implantation Technology IIT 2010*, AIP Conf. Proc. No. 1321 (AIP, New York, 2011), p. 83.

[5]M. Tanjyo, T. Nagayama, H. Onoda, N. Hamamoto, S. Umisedo, Y. Koga, H. Une, N. Maehara, Y. Kawamura, Y. Hashino, Y. Nakashima, M. Hashimoto, N. Tokoro, N. Nagai, K. Sekar, and W. Krull, in *Ion Implantation Technology 2010: 18th International Conference on Ion Implantation Technology IIT 2010*, AIP Conf. Proc. No. 1321 (AIP, New York, 2011), p. 105.

[6]J. Borland, J. Hautala, M. Gwinn, T. G. Tetreault, and W. Skinner, Solid State Technol. **47**, 64 (2004).

[7]E. Bourelle, A. Suzuki, A. Sato, T. Seki, and J. Matsuo, Nucl. Instrum. Methods Phys. Res., Sect. B **241**, 622 (2005).

[8]V. N. Popok, S. V. Prasalovich, and E. E. B. Campbell, Vacuum **76**, 265 (2004).

[9]S. Prasalovich, V. Popok, P. Persson, and E. E. B. Campbell, Eur. Phys. J. D **36**, 79 (2005).

[10]Y. Yamamura, Nucl. Instrum. Methods Phys. Res., Sect. B **33**, 493 (1988).

[11]V. I. Shulga, M. Vicanek, and P. Sigmund, Phys. Rev. A **39**, 3360 (1989).

[12]V. N. Popok, S. Vučković, J. Samela, T. T. Järvi, K. Nordlund, and E. E. B. Campbell, Phys. Rev. B **80**, 205419 (2009).

[13]V. N. Popok, J. Samela, K. Nordlund, and E. E. B. Campbell, Phys. Rev. B **82**, 201403(R) (2010).

[14]C. Raynaud, D. Tournier, H. Morel, and D. Planson, Diamond Relat. Mater. **19**, 1 (2010).

[15]A. D. Greentree, B. A. Fairchild, F. M. Hossain, and S. Prawer, Mater. Today **11**, 22 (2008).

[16]V. N. Popok, S. V. Prasalovich, M. Samuelsson, and E. E. B. Campbell, Rev. Sci. Instrum. **73**, 4283 (2002).

[17]S. Vučković, M. Svanqvist, and V. N. Popok, Rev. Sci. Instrum. **79**, 073303 (2008).

[18]K. Nordlund, M. Ghaly, R. S. Averback, M. Caturla, T. Diaz de la Rubia, and J. Tarus, Phys. Rev. B **57**, 7556 (1998).

[19]J. Tersoff, Phys. Rev. Lett. **61**, 2879 (1988).

[20]J. Tersoff, Phys. Rev. B **37**, 6991 (1988).

[21]J. F. Ziegler, J. P. Biersack, and M. D. Littmark, *The Stopping and Ranges of Ions in Matter* (Lulu, Morrisville, NC, 2008).

[22]K. Nordlund, J. Keinonen, and T. Mattila, Phys. Rev. Lett. **77**, 699 (1996).

[23]K. Nordlund, N. Runeberg, and D. Sundholm, Nucl. Instrum. Methods Phys. Res., Sect. B **132**, 45 (1997).

[24]V. N. Popok, J. Samela, K. Nordlund, and V. P. Popov, Nucl. Instrum. Methods Phys. Res., Sect. B, doi: 10.1016/j.nimb.2011.08.055.

[25]J. F. Prins, T. E. Derry, and J. P. F. Sellschop, Phys. Rev. B **34**, 8870 (1986).

[26]J. Samela and K. Nordlund, New J. Phys. **10**, 023013 (2008).

[27]T. Seki, T. Murase, and J. Matsuo, Nucl. Instrum. Methods Phys. Res., Sect. B **242**, 179 (2006).

[28]S. Pratontep, P. Preece, C. Xirouchaki, R. E. Palmer, C. F. Sanz-Navarro, S. D. Kenny, and R. Smith, Phys. Rev. Lett. **90**, 055503 (2003).

[29]J. R. Baker, Int. J. Impact Eng. **15**, 25 (1995).